

# Probing the braneworld hypothesis with a neutron-shining-through-a-wall experiment

Michaël Sarrazin,<sup>1,\*</sup> Guillaume Pignol,<sup>2</sup> Jacob Lamblin,<sup>2</sup>  
Fabrice Petit,<sup>3</sup> Guy Terwagne,<sup>4</sup> and Valery V. Nesvizhevsky<sup>5</sup>

<sup>1</sup>*Solid-State Physics Laboratory, Research Center in Physics of Matter and Radiation,  
University of Namur, 61 rue de Bruxelles, B-5000 Namur, Belgium*

<sup>2</sup>*LPSC, Université Grenoble-Alpes, CNRS/IN2P3, 53 rue des Martyrs, F-38026 Grenoble, France*

<sup>3</sup>*BCRC (Member of EMRA), 4 avenue du Gouverneur Cornez, B-7000 Mons, Belgium*

<sup>4</sup>*Laboratory of Analysis by Nuclear Reactions, Research Center in Physics of Matter and Radiation,  
University of Namur, 61 rue de Bruxelles, B-5000 Namur, Belgium*

<sup>5</sup>*Institut Laue-Langevin, 6 rue Jules Horowitz, F-38042 Grenoble, France*

The possibility for our visible world to be a 3-brane embedded in a multidimensional bulk is at the heart of many theoretical edifices in high-energy physics. Probing the braneworld hypothesis is thus a major experimental challenge. Following recent theoretical works showing that matter swapping between braneworlds can occur, we propose a *neutron-shining-through-a-wall* experiment. We first show that an intense neutron source such as a nuclear reactor core can induce a hidden neutron flux in an adjacent hidden braneworld. We then describe how a low-background detector can detect neutrons arising from the hidden world and quantify the expected sensitivity to the swapping probability. As a proof of concept, a constraint is derived from previous experiments.

PACS numbers: 11.25.Wx, 12.60.-i, 28.20.-v

## I. INTRODUCTION

As suggested by several extensions of the standard models of particle physics and cosmology, our world could form a three-dimensional space sheet (a brane) embedded in a larger bulk with more dimensions [1–3]. As for most theories beyond the Standard Model of particle physics, new effects predicted by the braneworld hypothesis at both the high-energy and the precision frontiers can be investigated. Particle colliders, such as the Large Hadron Collider, attempt to excite new degrees of freedom at high energies [4, 5] – like the Kaluza-Klein excitations of particles in the extra dimensions – whereas precision experiments at low energies attempt to find tiny signals induced by the new physics [6–17]. For instance, in the context of braneworld scenarios, the compactified extra dimensions would modify the inverse-square law of gravity at short distance. A great variety of experimental techniques have been developed to search for a possible modification of gravity from subatomic to macroscopic distance scales (see Ref. [6] for a recent review).

In the present work, we are interested in some peculiar low-energy effects induced by the existence of other branes in the bulk. In recent theoretical works [12–17], it has been argued that usual matter could leap from our braneworld to a hidden one, and vice versa (see Fig. 1). This matter swapping between two neighboring braneworlds could be triggered by magnetic vector potentials, either of astrophysical origin or generated experimentally. In particular, we have considered neutrons oscillating between a state where they sit in our brane and a state corresponding to a neutron located in the

other brane. The matter-swapping probability would oscillate at high frequency  $\eta$  and small amplitude  $p$ . Moreover, neutrons are well-known versatile tools which are already used to test other concepts such as axion [18] or mirror particles [19–23].

In a previous work, we have shown that such oscillations could have affected experiments measuring the neutron lifetime. The existing experiments set a constraint on anomalous neutron *disappearance* at the level of  $p < 7 \times 10^{-6}$  [17]. It is amusing to note that a small tension has very recently appeared between the neutron lifetimes measured with two different methods [24], which could be interpreted as anomalous neutron disappearance. In addition, such a constraint on neutron disappearance could also be useful to constrain some approaches related to the big bang nucleosynthesis [25].

In the present paper, we propose an experiment to investigate matter swapping between branes by looking at the *appearance* of neutrons from a neighboring brane. The concept is similar to *light-shining-through-a-wall* experiments (see Ref. [7] for a recent review of this topic) where photons from an intense light source would convert into a sterile state (dark photons or axion-like particles) which could pass through a wall, then would convert back to photons. In a *neutron-shining-through-a-wall* experiment, a very bright source of neutrons and a low-background neutron detector separated by a wall are necessary. Neutrons would swap into a sterile state – the state where they are located in another brane – which would be free to cross the wall. Then, the reappearance of neutrons into the detector situated behind the wall is checked. Although they are in principle very similar, there is an essential difference between light and neutrons shining through walls. As far as light is concerned, the oscillation frequency is supposed to be rather slow and the conversion of photons into a sterile state builds

---

\* michael.sarrazin@unamur.be

up coherently over long distance, while the oscillation is rather fast for neutrons and their conversion into sterile states results from the successive collisions of neutrons at nuclei.

In section II, the theoretical aspects and the phenomenology of the neutron dynamics in a two-brane universe at low energy are reviewed. The conditions leading to matter swapping between branes are given. The strength of the ambient magnetic vector potential (which drives the matter exchange between branes) is discussed, as well as the environmental conditions that could preclude the swapping to occur. In section III, we describe how the neutron diffusion in the reactor moderator creates a neutron flux in another brane and how this hidden neutron flux can be detected. Finally, the sensitivity of the suggested experiment is estimated, and as a proof of the concept, a constraint is derived from previous experiments.

## II. PHENOMENOLOGY OF BRANE MATTER SWAPPING

### A. Dynamics of swapping

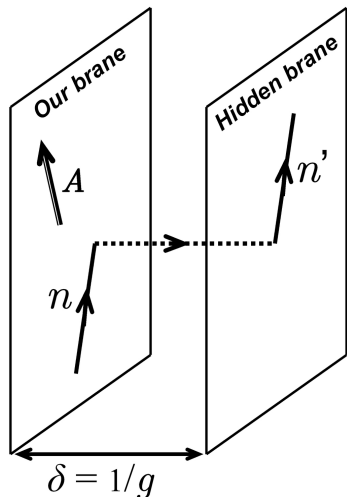


FIG. 1. Naive view of the neutron swapping between two branes. A neutron  $n$  in our brane can be transferred into a hidden brane (neutron  $n'$ ) under the influence of a suitable magnetic vector potential  $\mathbf{A}$ .  $g$  represents the coupling strength between the branes related to the effective distance  $\delta$  between each brane.

In previous works [12–15], it was shown that, in a universe containing two parallel braneworlds, the quantum dynamics of a spin-1/2 fermion in the presence of an electromagnetic field can be described by a two-brane Pauli equation at low energies. In electromagnetic and gravitational fields, the dynamics of a free neutron, i.e., outside of a nucleus, is described by the following equa-

tion [12–14]:

$$i\hbar \frac{\partial}{\partial t} \begin{pmatrix} \psi_+ \\ \psi_- \end{pmatrix} = (\mathbf{H}_0 + \mathbf{H}_{cm}) \begin{pmatrix} \psi_+ \\ \psi_- \end{pmatrix}, \quad (1)$$

where the indices  $\pm$  allow one to discriminate the two branes.  $\psi_+$  and  $\psi_-$  are usual Pauli spinors corresponding to the wave functions in the (+) and (-) branes, respectively. The unperturbed Hamiltonian  $\mathbf{H}_0$  is block diagonal and describes the usual nonrelativistic evolution of two uncoupled spin-1/2 fields in the magnetic fields  $\mathbf{B}_\pm$  and the gravitational potentials  $V_\pm$ , in each brane:

$$\mathbf{H}_0 = \begin{pmatrix} \mathbf{H}_+ & 0 \\ 0 & \mathbf{H}_- \end{pmatrix}, \quad (2)$$

$$\mathbf{H}_\pm = -\frac{\hbar^2}{2m} \Delta - \mu_n \boldsymbol{\sigma} \cdot \mathbf{B}_\pm + V_\pm. \quad (3)$$

The nondiagonal part  $\mathbf{H}_{cm}$  of the Hamiltonian describes the coupling between the branes,

$$\mathbf{H}_{cm} = g\mu_n \begin{pmatrix} 0 & -i\boldsymbol{\sigma} \cdot \{\mathbf{A}_+ - \mathbf{A}_-\} \\ i\boldsymbol{\sigma} \cdot \{\mathbf{A}_+ - \mathbf{A}_-\} & 0 \end{pmatrix}, \quad (4)$$

where  $\mathbf{A}_+$  and  $\mathbf{A}_-$  correspond to the magnetic vector potentials in the branes (+) and (-), respectively. The same convention is applied to the magnetic fields  $\mathbf{B}_\pm$  and to the gravitational potentials  $V_\pm$ .  $\mu_n$  is the magnetic moment of the neutron.  $\mathbf{H}_{cm}$  implies that matter exchange between branes depends on the magnetic moment and on the difference between the local (i.e., on a brane) values of the magnetic vector potentials.  $g$  is the coupling strength between the matter fields of each brane.

In the following section, the case of an ambient magnetic potential with an astrophysical origin is considered (section II B). Let  $\mathbf{A}_{amb} = \mathbf{A}_{amb,+} - \mathbf{A}_{amb,-}$  be the difference between the ambient magnetic potentials of each brane. Assuming that  $\mu_n B_\pm \ll V_\pm$ , i.e., the magnetic fields in the branes can be neglected (in particular assuming that  $\nabla \times \mathbf{A}_{amb} = \mathbf{0}$ ), then by solving the Pauli equation, the probability for a neutron initially localized in our brane to be found in the other brane is [12]

$$P = \frac{4\Omega^2}{\eta^2 + 4\Omega^2} \sin^2 \left( (1/2) \sqrt{\eta^2 + 4\Omega^2} t \right), \quad (5)$$

where  $\eta = |V_+ - V_-|/\hbar$  and  $\Omega = g\mu_n A_{amb}/\hbar$ .  $P$  is the instantaneous probability for matter swapping between branes. Equation (5) shows that the neutron in the potential  $A_{amb}$  undergoes Rabi-like oscillations between the branes. Note that the swapping probability is independent of the neutron spin direction [14]. As detailed in previous papers [14–16], the environmental interactions (related to  $V_\pm$ ) are usually strong enough and the oscillations are suppressed by the factor  $\Omega/\eta \ll 1$ . As a consequence, in a nucleus, a neutron is fully frozen in its brane due to the large nuclear potential.

## B. Ambient magnetic vector potential

The overall ambient astrophysical magnetic vector potential  $\mathbf{A}_{amb}$  was previously assessed in the literature [26].  $\mathbf{A}_{amb}$  is the sum of all of the magnetic vector potential contributions related to the magnetic fields of astrophysical objects (planets, stars, galaxies, etc.) since  $\mathbf{B}(\mathbf{r}) = \nabla \times \mathbf{A}(\mathbf{r})$ . As a rule of thumb,  $A \approx DB$  where  $D$  is the distance from the astrophysical source and  $B$  is the typical field induced by the object. At large distances from sources (for instance, close to the Earth),  $\mathbf{A}_{amb}$  is almost uniform (i.e.  $\nabla \times \mathbf{A}_{amb} \approx \mathbf{0}$ ) and cannot be canceled with magnetic shields [26]. Now, Eqs. (4) and (5) show the dependence of the swapping effect against  $\mathbf{A}_{amb} = \mathbf{A}_{amb,+} - \mathbf{A}_{amb,-}$ , i.e. the difference between the vector potentials of the two braneworlds. Since  $\mathbf{A}_{amb,-}$  depends on unknown sources in the hidden brane, we cannot assess its value. Then,  $\mathbf{A}_{amb}$  should be considered as an unknown parameter of the model. Nevertheless, the expected order of magnitude of  $A_{amb}$  can be roughly constrained by  $A_{amb,+}$  in our visible world (since  $A_{amb}$  results from a vectorial difference, it seems quite unlikely that  $A_{amb}$  can fortuitously fall to zero). Galactic magnetic field variations on local scales towards the Milky Way core ( $A_{amb} \approx 2 \times 10^9$  T m) are usually assumed [26]. By contrast, the Earth's magnetic field leads to 200 T m while the Sun contributes 10 T m [26]. By contrast, intergalactic contributions were expected to be about  $10^{12}$  T m [26] (see also our previous papers for a more detailed discussion [15–17]). Anyway, for now  $A_{amb}$  is a parameter fairly bounded between  $10^9$  T m and  $10^{12}$  T m.

## C. Environmental potential

If one considers free neutrons shielded from magnetic fields, only gravitational contributions are relevant. Because  $\eta = |V_+ - V_-|/\hbar$ , it is difficult to assess the value of  $\eta\hbar$  as it results from a scalar difference involving the unknown gravitational contribution  $V_-$  of the hidden world. Therefore,  $\eta$  appears as an effective unknown parameter of the model and could reach weak values of a few eV up to large values around 1 keV. Indeed, estimations given in previous works [15–17] suggest that  $V_+$  could be of the order of 500 eV due to the Milky Way core gravitational influence on neutrons. Note that the Sun, the Earth, and the Moon provide lower contributions of about 9 eV, 0.65 eV, and 0.1 meV, respectively. At last, it must be emphasized that  $\eta$  is time dependent due the motion of the Earth around the Sun at the lab scale. Between the Earth's aphelion and perihelion, the gravitational energy (due to the Sun) of a neutron varies from 9.12 to 9.43 eV. Of course, a time dependence could have many different origins. For instance, the particle motion relative to an unknown mass distribution in the hidden brane should be considered. However, it is unlikely that the Earth is "close" enough to a hidden mass distribution that is

large enough to induce a significant energy time dependence on a time scale of about one year or one day. The time dependence is then mainly induced by the Earth's motion around the Sun, with a relative variation in  $\eta$  of about 0.3‰ in one year. Such a variation could be detected through an annual modulation of the swapping probability (see section III D).

## D. Neutrons as a sensitive probe

With high-energy particle colliders, the braneworld hypothesis can be investigated if the brane thickness is in the range  $\xi \approx 10^{-19}$  m corresponding to the TeV scale ( $\hbar c/\xi \approx 1$  TeV). Colliders are blind to the Planck scale  $10^{-35}$  m. By contrast, experiments at lower energies using high-intensity neutron sources could reveal a multi-brane world through effects induced by the interbrane coupling  $g$ , which can be approximated by [12]

$$g \propto (1/\xi) \exp(-kd/\xi), \quad (6)$$

where  $d$  is the real distance between each brane in the bulk and  $k$  is a constant of the model [12]. Now, as an illustration, let us consider (for instance) a coupling constant  $g \approx 10^{-3} \text{ m}^{-1}$ . Such a value is consistent with present experimental bounds [17]. For branes at the TeV scale, the above value of  $g$  is reached for  $d \approx 50\xi$ . Now, if one considers branes at the Planck scale, the coupling constant remains unchanged for  $d \approx 87\xi$ . As a consequence, while brane physics could be invisible for colliders, it could be observed in low-energy experiments using neutrons if a second brane exists close enough to ours.

At last, we note that neutrons are more suitable than electrons, protons, or atoms for such a purpose [15]. Indeed, for a charged particle, the Hamiltonian (3) also contains the usual terms,

$$\mathbf{H}_{p,\pm} = -\frac{q}{m} \mathbf{A}_{\pm} \cdot \hat{\mathbf{P}} + \frac{q^2}{2m} |\mathbf{A}_{\pm}|^2, \quad (7)$$

with  $\hat{\mathbf{P}} = -i\hbar\nabla$ . This implies that the term  $\hbar\eta$  in Eq. (5) is then supplemented by large terms proportional to  $qA_{amb}$  which strongly freeze the oscillations. Considering, for instance,  $A_{amb} \approx 200$  T m (see section II B) and a proton with a kinetic energy of about 10 eV, the first term in the Hamiltonian (7) contributes 9 MeV to  $\hbar\eta$ . For such values, the amplitude of the oscillations is suppressed by 8 orders of magnitude compared to the neutron case. Now, let us consider atoms. Though they are neutral, atoms are endowed with an instantaneous electric dipole moment (IEDM)  $\mathbf{d}$ . Obviously, according to the time average, we must verify that  $\langle \mathbf{d} \rangle = \mathbf{0}$  and  $\langle \mathbf{d}^2 \rangle \neq \mathbf{0}$  since IEDM results from quantum fluctuations of atomic orbitals. The London dispersion forces between atoms result from interactions between these instantaneous dipoles. Then, the Hamiltonian (3) must be

supplemented by terms which derive from Eq. (7):

$$\mathbf{H}_{d,\pm} \sim -\mathbf{A}_{\pm} \cdot \frac{\Delta \mathbf{d}}{\Delta t}, \quad (8)$$

where the fluctuation time is about  $\Delta t \sim \hbar/E_i$ , where  $E_i$  is the ionization energy of the atom ( $E_i \approx 10$  eV). Provided that  $\Delta t$  is larger than the period  $T$  of the Rabi oscillation of an atom between two branes,  $\hbar\eta$  in Eq. (5) is then supplemented by a huge term proportional to  $(1/\Delta t)\mathbf{A}_{amb} \cdot \mathbf{d}$ . Then, for  $d$  about  $10^{-30}$  C·m (0.3 D) (a typical value for atoms) and  $A_{amb} \approx 200$  T m only (for instance), we still get  $\hbar\eta \approx 20$  MeV. With these values, the oscillations are strongly damped by 9 orders of magnitude compared to the neutron case. As a result, the neutron is a good candidate to test matter swapping between branes, since it is devoid of global charge or any electric dipole moment.

### E. Collision-induced neutron swapping probability

As a consequence of the environmental potential  $\eta\hbar$ , the neutron oscillations present weak amplitude and high angular frequency of the order  $\eta/2$ . Due to the fast oscillating behavior, one can approximate the swapping probability by its time-averaged value  $p = \langle P \rangle$  (see Eq. (5)), such that

$$p = \frac{2\Omega^2}{\eta^2}. \quad (9)$$

When freely propagating, the neutron can be described as a superposition of two states: a neutron in our brane vs a neutron in the other brane. When colliding with a nucleus situated in our brane, the interaction acts as a measurement and the neutron collapses either in our brane with a probability  $1 - p$  or in the other invisible brane with a probability  $p$ . In the following sections, the swapping probability  $p$  is considered as the relevant measurable parameter. By contrast, bounds on the coupling parameter  $g$  depend on the knowledge of galactic magnetic potential fields and on the ambient gravitational fields.

## III. A NEUTRON-SHINING-THROUGH-A-WALL EXPERIMENT

As explained above, in a two-brane universe, neutrons have a nonzero probability to escape from our brane into another brane at each collision. Therefore, a nuclear reactor, where the neutron density is very high, would be a very intense source of hidden neutrons. These neutrons could escape the reactor and be detected, after having swapped back to our brane, with a standard neutron detector located near the reactor (see Fig. 2). In the present section, the expected magnitude of the hidden

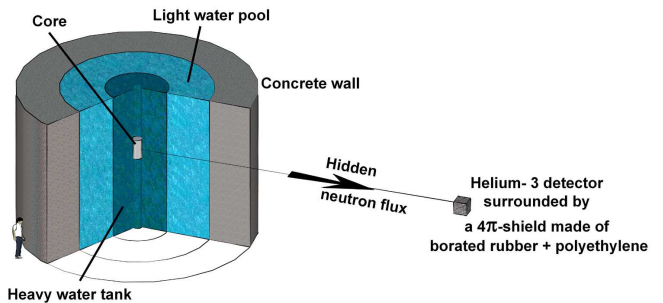


FIG. 2. Sketch of the experimental device. The source of possible hidden neutrons is a nuclear reactor core (here for instance, the Institut Laue-Langevin facility in Grenoble, France). The neutron detector using helium-3 gas is considered to detect neutrons which could emerge from a hidden world. The detector is embedded in a shield to reach a very low background.

neutron flux as a function of the swapping probability is discussed and the sensitivity which can be reached with such an experiment is estimated. For sake of clarity, the details of our calculations only appear in the Appendices.

### A. Induced neutron flux in the hidden world

Let us assume that our Universe is made of two mutually invisible braneworlds and let us also consider a neutron flux  $\Phi_+$  inside a nuclear core. Our aim is to determine the intensity of the hidden neutron flux  $\Phi_-$  (in the vacuum of the hidden braneworld) in the core vicinity. For a given volume element of the reactor, since each neutron collision creates a hidden neutron with probability  $p$ , the hidden neutron source is proportional to the macroscopic elastic cross section  $\Sigma_E$  of the reactor moderator and to the neutron flux  $\Phi_+$ . More specifically, we get the source term corresponding to the number of generated hidden neutrons per unit volume and unit time (see Appendix A):

$$S_- = \frac{1}{2}p\Sigma_E\Phi_+, \quad (10)$$

where  $p$  is given by Eq. (9). Equation (10) is derived by using the matrix density approach [27, 28] related to Eq. (1) as shown in Appendix A. From this source term, we deduce the hidden neutron flux  $\Phi_-$  at the position  $\mathbf{r}$  by considering the solid angle and integrating over the reactor volume  $V$ :

$$\Phi_-(\mathbf{r}) = \frac{p}{8\pi} \int_V \frac{1}{|\mathbf{r} - \mathbf{r}'|^2} \Sigma_E(\mathbf{r}') \Phi_+(\mathbf{r}') d^3r'. \quad (11)$$

The relation (11) shows that any signal should decay as  $1/D^2$  when the distance  $D$  between the reactor and the detector increases. This is an important issue to discriminate a hidden neutron signal from the common

neutron background in the reactor vicinity. Indeed, such a background mainly depends on local secondary sources.

### B. Principle of hidden neutron flux detection

We now want to build a detector that is able to measure the hidden neutron flux. Neutron detectors are based on the detection of charged particles emitted after neutron absorption. In the present case, we suggest the use of a gaseous detector, such as the usual helium-3 or boron trifluoride ( $\text{BF}_3$ ) neutron detectors. The mechanism of hidden neutron capture can be described through the approach of Feinberg and Weinberg [27], which was also used by Demidov, Gorbunov, and Tokareva [28] to describe the positronium oscillations in a volume full of gas in the mirror matter concept. Details of the calculation are shown in Appendix B. We can then compute the event rate  $\Gamma$  detected in our brane against the swapping probability  $p$  (see Appendix B). For monochromatic neutrons, we get the intuitive but not obvious result

$$\Gamma = \frac{1}{2}p\Sigma_A\Phi_-V, \quad (12)$$

where  $V$  is the volume of the detector and  $\Sigma_A$  is the macroscopic absorption cross section related to  $\text{BF}_3$  or He-3. For a continuous energy spectrum, the event rate is obtained by integrating Eq. (12) over the spectrum. The main difficulty comes from the background which is usually high in such an environment. The detector must be shielded from neutrons.

### C. Proposal at the ILL reactor

For our experiment, we propose to use the Institute Laue-Langevin (ILL) reactor (see Fig. 2) where the core (diameter of 40 cm and height of 80 cm) is surrounded by a heavy water tank (diameter of 2.5 m and height of 2 m) which will be our hidden neutron source. It can be shown that the major contribution to the hidden neutron flux comes from the heavy water tank, while neutrons are strongly absorbed by light water and other surrounding materials. The thermal neutron flux inside the heavy water tank is modeled by using a point-like source  $\Phi_+(r) = S \exp(-r/L)/(4\pi Dr)$ , where  $L = 116$  cm and  $D = 0.57$  cm are the length and coefficient of diffusion for heavy water, respectively.  $S$  is fitted to match with the known neutron flux in the heavy water tank [29] with  $S = 6.0 \times 10^{17}$  neutrons/s. For heavy water, the macroscopic elastic cross section is  $\Sigma_E = 0.4 \text{ cm}^{-1}$ . The present rough model is reliable enough to discuss the experimental concept. Indeed, it is sufficient to assess the correct magnitude of the induced hidden neutron flux. Of course, any discussion of the later experimental

results will require a detailed computation of the neutron flux in each location inside of the reactor, as well as a consideration of the various materials surrounding the core.

We plan to use a cylindrical helium-3 detector (see Fig. 2) with a volume of  $36 \text{ cm}^3$  and a gas pressure of 4 atm. This detector could be located at 10 meters from the center of the core. The detector will be shielded by a  $4\pi$ -box made of a (at least) 3-cm thick borated rubber (40% boron content) to capture thermal neutrons, supplemented by a polyethylene cover with a tunable thickness to moderate epithermal and fast neutrons. Indeed, hidden neutrons should provide a characteristic constant counting rate which does not depend on the shielding thickness.

Using Eqs. (11) and (12), the estimated rates are shown in Fig. 3 (black solid line). Considering the previous constraint  $p < 7 \times 10^{-6}$  [17] (vertical blue solid line), we see that the expected event rate could be as high as 36 kHz, which is easily detectable even without shielding. Actually, we think we can reach an upper rate of about 10 mHz or even 1 mHz [30–32] with suitable shields and detector (horizontal red solid line). We can then expect to reach a new upper constraint for the swapping probability  $p$  of about  $10^{-9}$ . Such a constraint would be better than the constraint  $p < 7 \times 10^{-6}$  [17] by at least 3 orders of magnitude.

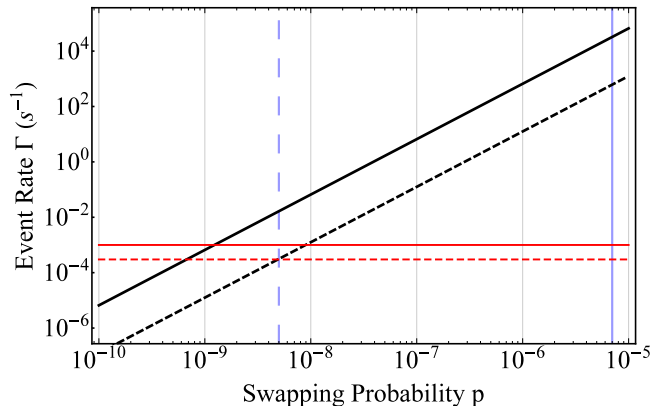


FIG. 3. (Color online). Black solid line: Expected event rate  $\Gamma$  against the swapping probability  $p$ . Horizontal red solid line: Expected threshold of the background noise (1 mHz). Vertical blue solid line: Known upper limit of the constraint on the swapping probability  $p < 7 \times 10^{-6}$  [17]. Black dashed line: Expected event rate  $\Gamma$  against the swapping probability  $p$  by considering the experiment in Ref. [30]. Horizontal red dashed line: Background noise (0.3 mHz) in the experiment in Ref. [30]. Vertical blue dashed line: Threshold of the rough constraint on the swapping probability ( $p < 5 \times 10^{-9}$ ) considering the experiment in Ref. [30].

In Fig. 4, as an example, we show the resulting expected bound on the coupling constant  $g$  between our brane and an invisible one. The values of  $g$  are given against the gravitational constraint  $\eta$  from Eq. (9). The existing constraint is given [17] (shaded domain above the

short-dashed blue line) and is compared to the expected results of the neutron-shining-through-a-wall experiment (black solid line) by assuming  $A_{amb} \approx 2 \times 10^9$  T m [17]. For the best rate constraint, we improve the constraint on  $g$  by 2 orders of magnitude. By contrast, a constraint on the detected signal lower than 10 events per second (see Fig. 3) still allows  $p < 10^{-7}$ , i.e., we improve the constraint on  $g$  by 1 order of magnitude. As a consequence, the present experiment can easily improve the constraint on the coupling between our world and invisible ones.

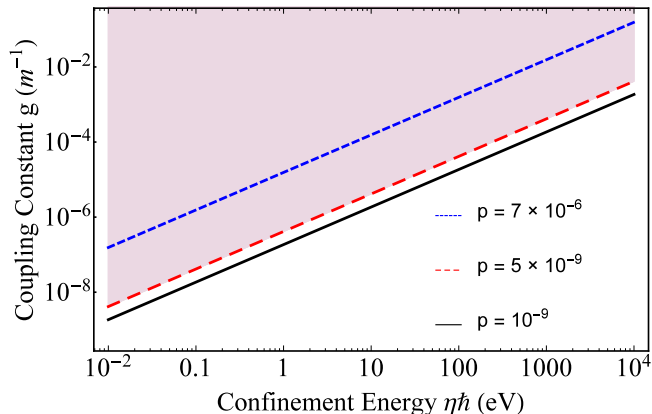


FIG. 4. (Color online). Expected experimental limits for the coupling constant  $g$  against the confinement energy for some constraints on the swapping probability  $p$  for  $A_{amb} = 2 \times 10^9$  T m. Red-grey domains are excluded.  $p = 7 \times 10^{-6}$  corresponds to our previous best experimental constraint.  $p = 5 \times 10^{-9}$  corresponds to the expected constraint deduced from the experiment in Ref. [30].

#### D. Yearly time-dependent drift of the swapping probability

Let us now briefly underline the possible consequence of the potential  $\eta\hbar$  time evolution due to the Earth's revolution around the Sun, as described in section II C. From Eq. (9)  $p$  varies in time as  $\Delta p/p = 2\Delta\eta/\eta$ . Now, from Eqs. (11) and (12)  $\Gamma$  varies as  $\Delta\Gamma/\Gamma = 2\Delta p/p$ . Then, we deduce that the event rate  $\Gamma$  varies in time as  $\Delta\Gamma/\Gamma = 4\Delta\eta/\eta$ , i.e.,  $\Delta\Gamma/\Gamma \approx 10^{-3}$  over six months if we consider the values from section II C. If it is expected to detect a time-dependent drift of the swapping probability, for a given duration  $\Delta t$  of the experiment, the number of detected neutrons  $N = \Gamma\Delta t$  and its instrumental uncertainty  $\Delta N \sim \sqrt{N}$  imply that enough neutrons must be detected to allow  $\Delta N/N$  to be lower than  $4\Delta\eta/\eta$ . In the present case, for month-by-month measurements, we should have  $N > 10^6$  detected neutrons per month at least. Assuming  $\Delta t \sim 20$  days per month, this leads to  $\Gamma \approx 1$  Hz. As a consequence, considering the above-mentioned detector, a time-dependent drift of the swapping probability  $p$  can be measured provided that  $p > 3.7 \times 10^{-8}$ .

#### E. A constraint as a proof of concept

A constraint can be suggested from previous experiments [30–32]. Indeed, in different contexts, these experiments required low-noise neutron detectors to detect ultracold neutrons generated by conventional sources. But since these detectors were in the nuclear reactor neighborhood, they should have been sensitive to hidden neutrons as well. As a consequence, considering the recorded background of these experiments, we can already derive a first rough constraint on the swapping probability, and thus on the coupling constant between two adjacent branes. We consider the favorable conditions introduced in Ref. [30]. The detector volume was  $500 \text{ cm}^3$  with a partial helium-3 pressure of 15 mbar. The distance between the detector and the nuclear core was 16.5 m. The background was 0.3 mHz [30]. The resulting constraint is shown in Fig. 3. Using the previously introduced reactor model, the expected hidden neutron flux  $\Gamma$  against the swapping probability  $p$  is shown by the black dashed line. The neutron background is shown by the horizontal red dashed line. As a result, this leads to a new constraint for the swapping probability  $p$  such that (see vertical blue dashed line in Fig. 3)

$$p \leq 5 \times 10^{-9}. \quad (13)$$

Such a value can be related to a constraint on the coupling constant between our visible braneworld and a hypothetical invisible one. This constraint is given by the red dashed line in Fig. 4. Obviously, these constraints need to be confirmed or improved by a dedicated experiment such as that described in the previous sections. As a consequence, the present constraint on  $p$  does not preclude the measurement of a yearly time-dependent drift of the swapping probability. Nevertheless, it shows the feasibility of the experiment introduced in the present work.

#### IV. CONCLUSION

We have proposed an experiment in which neutrons can be used to test the braneworld hypothesis. Using an intense flux of neutrons behind a wall and utilizing a properly shielded neutron detector, reappearing neutrons could be detected as a proof of the existence of hidden braneworlds. Three typical signatures can be examined to verify the reliability of a measured signal as a real exotic phenomenon. First, for thick enough shielding, the number of detected neutrons must not depend on the shield thickness. Second, when the distance to the core increases, the number of detected neutrons must decay as an inverse-square law against the distance between the nuclear core and the detector. At last, a yearly modulated time-dependent drift of the number of detected neutrons could be observed for a not too low

swapping probability. By contrast, without direct detection, such an experiment at least allows one to constrain the existence of braneworlds. The experimental constraint on the matter-swapping probability between branes could be improved by 3 orders of magnitude with the proposed experiment. Then, a rough constraint on the swapping probability was proposed to show the feasibility of a neutron-shining-through-a-wall experiment.

### ACKNOWLEDGMENTS

The authors thank Karin Derochette for critical reading of the manuscript.

### Appendix A: Shielded nuclear core as a hidden neutron source

In a previous work [17], it was shown that ultracold neutrons colliding with a solid wall can escape to another hidden brane. In this situation, since ultracold neutrons present a wavelength roughly larger than the typical distance between atoms of the wall, the wall appears as a continuous medium for neutrons [33]. Such a medium can be described through the Fermi potential [33]. Here, we want to estimate the production rate of hidden neutrons due to collisions between fast (or thermal) neutrons and materials surrounding the nuclear core, i.e. mainly the heavy and light water tanks. In this context, since neutrons cannot be considered in the "optical" domain, the media cannot be considered as continuous, and we must consider collisions between neutrons and individual nuclei. Then, our aim is to find a relation between the visible neutron flux  $\Phi_+$  and the hidden neutron flux  $\Phi_-$  induced by the collisions between visible neutrons and nuclei in our brane. More specifically, we look for a source term,

$$S_- = K\Phi_+, \quad (\text{A1})$$

where the constant  $K$  in the source term will be assessed in the following. It will be shown that  $K = (1/2)p\Sigma_E$ , where  $\Sigma_E$  is the macroscopic elastic cross section of the materials of the reactor and  $\Phi_+$  is the neutron flux in the whole reactor. To do this, considering the matrix density approach, we follow the Feinberg-Weinberg approach [27], which was also used by Demidov, Gorbunov, and Tokareva [28] to describe other kinds of oscillations in a volume occupied by matter.

Neutrons are described through the two-brane Pauli equation and we neglect the neutron decay process:

$$i\hbar\partial_t\Psi = \mathbf{H}\Psi, \quad (\text{A2})$$

such that

$$\mathbf{H} = \begin{pmatrix} -\frac{\hbar^2}{2m}\Delta + V_{g,+} & -ig\mu_n\sigma \cdot \mathbf{A}_{amb} \\ ig\mu_n\sigma \cdot \mathbf{A}_{amb} & -\frac{\hbar^2}{2m}\Delta + V_{g,-} \end{pmatrix}, \quad (\text{A3})$$

where  $V_{g,+}$  and  $V_{g,-}$  are the gravitational potentials felt by the neutron in each brane. We assume that  $\sigma \cdot \mathbf{A}_{amb} = A_{amb}\sigma_z$  and we restrain ourselves to a spin-up state without loss of generality (the matter-swapping probability does not depend on the direction of the magnetic vector potential or the spin state [13–15]). Then we can write

$$\mathbf{H} = \begin{pmatrix} -\frac{\hbar^2}{2m}\Delta + V_{g,+} & -i\Omega\hbar \\ i\Omega\hbar & -\frac{\hbar^2}{2m}\Delta + V_{g,-} \end{pmatrix}, \quad (\text{A4})$$

with  $\Omega\hbar = g\mu_n A_{amb}$ . The behavior of the neutron flux is described through the use of the matrix density  $\rho$  [27],

$$\frac{d}{dt}\rho = -i\hbar^{-1}(\mathcal{H}\rho - \rho\mathcal{H}^\dagger) + I_c, \quad (\text{A5})$$

where  $I_c$  is the collisional integral which describes the collisions between neutrons and nuclei in the medium, with

$$I_c = nv \int F(\theta)\rho F^\dagger(\theta)d\Omega. \quad (\text{A6})$$

$v$  is the mean relative velocity between neutrons and molecules and  $n$  is the density of molecules (nuclei) in matter. We have

$$F(\theta) = \begin{pmatrix} f(\theta) & 0 \\ 0 & 0 \end{pmatrix}, \quad (\text{A7})$$

which describes the scattering of neutrons by the molecules and where  $\theta$  is a scattering angle. The second diagonal term is equal to zero since we assume there is no matter in the hidden brane.

We also define  $\mathcal{H} = \mathbf{H} + \mathbf{C}$ , with

$$\mathbf{C} = \begin{pmatrix} -2\pi nv\hbar f(0)/k & 0 \\ 0 & 0 \end{pmatrix}, \quad (\text{A8})$$

(where  $k$  is the neutron wave vector), which accounts for the presence of matter in the system. Let us use the definition

$$\rho = \begin{pmatrix} \rho_+ & r + is \\ r - is & \rho_- \end{pmatrix}. \quad (\text{A9})$$

We also define

$$w_R = 4\pi\frac{nv}{k}\text{Re}(f(0)), \text{ and } w_I = 4\pi\frac{nv}{k}\text{Im}(f(0)) \quad (\text{A10})$$

with the optical theorem related to the cross section  $\sigma_{tot}$ :

$$\sigma_{tot} = \sigma_E + \sigma_I = \frac{4\pi}{k}\text{Im}(f(0)) = \frac{w_I}{nv}, \quad (\text{A11})$$

where  $\sigma_E$  and  $\sigma_I$  are the elastic and inelastic (absorption) cross sections, and

$$\sigma_E = \int |f(\theta)|^2 d\Omega. \quad (\text{A12})$$

We then obtain the following system from Eq. (A5):

$$\frac{d}{dt}\rho_+ = -2\Omega r - nv\sigma_I\rho_+, \quad (\text{A13})$$

$$\frac{d}{dt}\rho_- = 2\Omega r, \quad (\text{A14})$$

$$\frac{d}{dt}r = (\eta - (1/2)w_R)s - (1/2)rw_I + \Omega(\rho_+ - \rho_-), \quad (\text{A15})$$

$$\frac{d}{dt}s = -(\eta - (1/2)w_R)r - (1/2)sw_I, \quad (\text{A16})$$

with  $\hbar\eta = V_{g,+} - V_{g,-}$ . In the following, we consider a statistical set of neutrons initially localized in our visible brane and emerging from the nuclear core, i.e.,  $\rho_+(t=0) = 1$  and  $\rho_-(t=0) = 0$ . If we consider Eq. (A13), we obviously deduce that the neutron population in our brane must mainly decrease due to absorption, i.e., neutron leakage into a hidden brane must be very weak to be consistent with known physics. So, we must verify that  $2\Omega r \ll nv\sigma_I\rho_+$ . Now, if (for instance) we consider thermal neutrons in heavy water, and if we consider  $\Omega$  with  $A_{amb} = 2 \times 10^9$  T m and  $g = 10^{-3}$  m<sup>-1</sup>, we get  $nv\sigma_I \approx 7.3$  s<sup>-1</sup> and  $\Omega \approx 2 \times 10^{14}$  s<sup>-1</sup>, i.e.,  $2\Omega \gg nv\sigma_I$ . As a consequence, the previous condition must imply that  $r \ll \rho_+$ . Since neutron leakage must be weak, we also deduce that  $\rho_- \ll \rho_+$ . At last, assuming that  $\eta \gg w_R$  and using Eq. (A11), Eqs. (A13)-(A16) can be recast in the following convenient form:

$$\frac{d}{dt}\rho_+ = -nv\sigma_I\rho_+, \quad (\text{A17})$$

$$\frac{d}{dt}\rho_- = 2\Omega r, \quad (\text{A18})$$

$$\frac{d}{dt}r = \eta s - (1/2)nv\sigma_{tot}r + \Omega\rho_+, \quad (\text{A19})$$

$$\frac{d}{dt}s = -\eta r - (1/2)nv\sigma_{tot}s. \quad (\text{A20})$$

At this stage of the problem, it is relevant to underline that from Eqs. (A19) and (A20) we can easily deduce

$$\frac{d}{dt}m = -(1/2)nv\sigma_{tot}m + \Omega \cos\theta\rho_+, \quad (\text{A21})$$

where we have set  $r + is = me^{i\theta}$ . Without coupling, i.e., if  $\Omega = 0$ , we deduce from Eq. (A21) that the coherence terms of the density matrix (i.e., its off-diagonal terms  $r$  and  $s$ ) must exponentially decay as  $\exp(-(1/2)nv\sigma_{tot}t)$ . As a consequence, the collisional dynamics should suppress the quantum coherence precluding the neutron swapping between branes. By contrast, Eq. (A21) as well as Eqs. (A19) and (A20) also show us that the coupling

$\Omega$  can prevent decoherence. This allows stationary coherences such that  $dr/dt = ds/dt = 0$ , with  $r$  and  $s$  different from zero. The steady state is quickly achieved due to the above-mentioned exponential behavior. Let us call  $X$  the distance covered by the neutron in the medium. The length  $X$  cannot be equated to the crossed thickness  $L$  in the medium. Since neutrons are localized in our visible brane, they can be diffused by molecules or the nuclei of atoms.  $X$  is the sum of the lengths of the various straight lines covered by the neutron, and thus  $L = X\sqrt{\sigma_I/3\sigma_E}$ . Now, for instance, since  $n\sigma_{tot} \approx 0.4$  cm<sup>-1</sup> for heavy water, the stationary coherences occur at  $X = 4$  cm, i.e.,  $L = 0.2$  mm from the neutron source, a distance which must be compared to the 105-cm thick heavy water slab in the ILL's reactor. By contrast,  $n\sigma_I = 4 \times 10^{-5}$  cm<sup>-1</sup> in D<sub>2</sub>O, i.e.,  $\rho_+$  slowly varies in the heavy water region (see Eq. (A17)). Then, in the stationary coherences hypothesis, Eqs. (A19) and (A20) become a linear system of two equations with two unknowns ( $r$  and  $s$ ) which is trivially solved. We get

$$\begin{pmatrix} r \\ s \end{pmatrix} = \frac{1}{(1/4)(nv\sigma_{tot})^2 + \eta^2} \begin{pmatrix} (1/2)nv\sigma_{tot}\Omega\rho_+ \\ -\eta\Omega\rho_+ \end{pmatrix}. \quad (\text{A22})$$

From Eqs. (A18) and (A22) we deduce

$$\frac{d}{dt}\rho_- \approx (1/2)pnv\sigma_{tot}\rho_+, \quad (\text{A23})$$

where we have set  $p = 2\Omega^2/\eta^2$  to be consistent with Eq. (9). Let us now consider an initial local neutron flux  $\Phi_0 = u_0v$  where  $u_0$  is the initial neutron density. The neutron fluxes in each brane are given by  $\Phi_{\pm} = \Phi_0\rho_{\pm}$ . Then, from Eq. (A23) we deduce

$$\partial_t\Phi_- = (1/2)pnv\sigma_{tot}\Phi_+. \quad (\text{A24})$$

Since the neutron flux  $\Phi_- = u_-v$ , where  $u_-$  is the local neutron density in the hidden brane, then

$$\partial_t u_- = (1/2)pn\sigma_{tot}\Phi_+. \quad (\text{A25})$$

Since  $u_-$  is now local, Eq. (A25) must be supplemented by a divergence term  $\nabla \cdot \mathbf{j}_-$  to account for the local behavior of the neutron current  $\mathbf{j}_- = u_- \mathbf{v}$ . We then deduce the continuity equation for neutrons in the second brane,

$$\nabla \cdot \mathbf{j}_- + \partial_t u_- = (1/2)pn\sigma_{tot}\Phi_+, \quad (\text{A26})$$

which is the continuity equation endowed with a source term  $S_-$ ,

$$S_- = (1/2)pn\sigma_{tot}\Phi_+. \quad (\text{A27})$$

Obviously, for heavy water,  $\sigma_{tot} \approx \sigma_E$  and we retrieve Eq. (A1) since  $n\sigma_E = \Sigma_E$ . Now, as a striking result, we note that neutrons propagating in the hidden brane are not absorbed since we expect vacuum rules in the



other world. As a consequence, while visible neutrons have been stopped by the water surrounding the nuclear core, hidden neutrons can propagate freely far away from the reactor. Then we can completely suppress the visible neutron flux in our brane while keeping a constant flux of hidden neutrons in the invisible brane. A hidden neutron source from a nuclear core surrounded by a relevant shield can then be built.

## Appendix B: Hidden neutron detector

We consider a gas stored in a vessel as a neutron detector. More specifically, we consider a neutron flux in the second brane and we expect to detect neutrons which arise from the second brane in our braneworld. The distance between the atoms in the gas is much larger than the neutrons' wavelength. As a consequence, neutrons see a set of scattering objects instead of a continuous medium. We follow the same approach as before, and start with Eqs. (A13) to (A16), but now we consider a statistical set of neutrons initially localized in the invisible brane, such as it can be written  $\rho_+(t=0) = 0$  and  $\rho_-(t=0) = 1$ .

Looking at Eq. (A14), we see that the neutron population in the hidden brane mainly decreases due to neutron leakage into a hidden brane. Following a similar hypothesis as in the previous section, we can consider that  $2\Omega r$  must be very weak and we assume that  $\partial_t \rho_- \approx 0$ , i.e.,  $\rho_-$  is almost constant at the detector scale. We can also assume that  $\rho_+ \ll \rho_-$  and  $\eta \gg w_R$ . Then (using Eq. (A11)), Eqs. (A13)-(A16) can be recast in the following convenient form:

$$\frac{d}{dt}\rho_+ = -2\Omega r - nv\sigma_I\rho_+, \quad (\text{B1})$$

$$\rho_- \approx 1, \quad (\text{B2})$$

$$\frac{d}{dt}r = \eta s - (1/2)rnv\sigma_{tot} - \Omega\rho_-, \quad (\text{B3})$$

$$\frac{d}{dt}s = -\eta r - (1/2)snv\sigma_{tot}. \quad (\text{B4})$$

Obviously,  $\sigma_{tot}$ ,  $\sigma_I$ , and  $\sigma_E$  are now the cross sections related to the gas and  $n$  is the density of gas molecules.

Now, from Eqs. (B3) and (B4) we can easily deduce that

$$\frac{d}{dt}m = -(1/2)nv\sigma_{tot}m - \Omega \cos\theta\rho_-, \quad (\text{B5})$$

where  $r + is = me^{i\theta}$  is set. Without coupling, i.e., if  $\Omega = 0$ , we deduce from Eq. (B5) that the coherence terms of the density matrix (i.e., its off-diagonal terms  $r$  and  $s$ ) must exponentially decay as  $\exp(-(1/2)nv\sigma_{tot}t)$ . As a consequence, the collisional dynamics should suppress the quantum coherence precluding the neutron swapping between branes. By contrast, Eq. (B5) as well as Eqs. (B3) and (B4) also show that the coupling  $\Omega$  preserves from decoherence. Nevertheless, in contrast to the case described in the previous section, stationary coherences such that  $dr/dt = ds/dt = 0$  (with  $r$  and  $s$  different from zero) cannot be achieved here due to the short length of the detector. Indeed, assuming for instance a He-3 detector with a pressure of about 4 atm, we get  $n\sigma_{tot} \approx 0.53 \text{ cm}^{-1}$  for thermal neutrons. Now, the distance  $X = vt$  crossed by a neutron can be equated to the length  $L$  of the detector since we can assume that the hidden neutrons are not significantly diffused by the nuclei of gas molecules or atoms in our brane. Let us consider (for instance) a detector length of about 10 cm. At half length, we get  $\exp(-(1/2)nv\sigma_{tot}t) \approx 27 \%$ , i.e., the coherences are not negligible in at least half of the detector. As a consequence, we cannot apply the stationary coherences hypothesis here.

Nevertheless, Eqs.(B3) and (B4) constitute a simple nonhomogeneous first-order differential equation that is easy to solve since  $\rho_- \approx 1$ , i.e., since  $\rho_-$  is constant. Let us set

$$\begin{pmatrix} r \\ s \end{pmatrix} = e^{-(1/2)nv\sigma_{tot}t} \begin{pmatrix} \cos(\eta t) & \sin(\eta t) \\ -\sin(\eta t) & \cos(\eta t) \end{pmatrix} \begin{pmatrix} R \\ S \end{pmatrix}. \quad (\text{B6})$$

If we insert Eq. (B6) into Eqs.(B3) and (B4), we obtain

$$\frac{d}{dt} \begin{pmatrix} R \\ S \end{pmatrix} = e^{(1/2)nv\sigma_{tot}t} \begin{pmatrix} \cos(\eta t) & -\sin(\eta t) \\ \sin(\eta t) & \cos(\eta t) \end{pmatrix} \begin{pmatrix} -\Omega\rho_- \\ 0 \end{pmatrix}, \quad (\text{B7})$$

from which we deduce that

$$\begin{pmatrix} R \\ S \end{pmatrix} = -\Omega\rho_- \begin{pmatrix} \int_0^t \cos(\eta t') e^{(1/2)nv\sigma_{tot}t'} dt' \\ \int_0^t \sin(\eta t') e^{(1/2)nv\sigma_{tot}t'} dt' \end{pmatrix}. \quad (\text{B8})$$

Using Eqs.(B6) and (B8), Eq. (B1) can be rewritten as

$$\frac{d}{dt}\rho_+ = 2\Omega^2\rho_- \int_0^t e^{-(1/2)nv\sigma_{tot}(t-t')} \cos(\eta(t-t')) dt' - nv\sigma_I\rho_+, \quad (\text{B9})$$

which leads to

$$\rho_+ = 2\Omega^2 \rho_- \int_0^t \int_0^{t'} e^{-(1/2)nv\sigma_{tot}(t'-t'')} e^{-nv\sigma_I(t-t')} \cos(\eta(t' - t'')) dt'' dt'. \quad (\text{B10})$$

From the properties of the density matrix  $\rho$ , we can deduce the emerging neutron flux  $\Phi_v$  which can be detected from the hidden current:  $\Phi_v = \Phi_- \rho_+$ . Considering He-3 mixtures or BF<sub>3</sub>, we assume that the inelastic cross section  $\sigma_I$  stands for the neutron capture probability and the production of protons, which can be recorded. Then, the rate  $\Gamma$  of events recorded per second by the detector in our brane is given by

$$\begin{aligned} \Gamma &= \int_0^{L/v} nv\sigma_I \int_{S_d} \Phi_v dS dt \quad (\text{B11}) \\ &= \int_0^{L/v} nv\sigma_I \rho_+ \int_{S_d} \Phi_- dS dt, \end{aligned}$$

Assuming that  $\eta \gg nv\sigma_{tot}$ , and setting  $p = 2\Omega^2/\eta^2$  and  $x = vt$ , from Eqs. (B10) and (B11) we get

$$\Gamma = \varphi_s p \frac{n\sigma_I \eta^2}{v^2} \int_0^L e^{-n\sigma_I x} \int_0^x \int_0^{x'} e^{(1/2)n\sigma_{tot}(x''-x')} e^{n\sigma_I x'} \cos((\eta/v)(x'' - x')) dx'' dx' dx \quad (\text{B12})$$

with  $\varphi_s = \int_{S_d} \Phi_- dS$ .

Due to the fast oscillating cosine term, and since  $\eta \gg nv\sigma_{tot}$ , Eq. (B12) reduces to

$$\Gamma \sim (1/2)\varphi_s p \left[ \left( \frac{\sigma_E}{\sigma_I} - 1 \right) (e^{-n\sigma_I L} - 1) + n\sigma_{tot} L \right]. \quad (\text{B13})$$

For pure helium-3, relevant argon-helium-3 mixtures, or BF<sub>3</sub>, we verify that  $\sigma_I \gg \sigma_E$ , and then for long enough

where  $S_d$  is the effective area of the detector and  $L$  is the length of the gas vessel, such that  $L/v$  is the time during which hidden neutrons travel in the detector volume. The length  $L$  can be equated to the length of the detector since we can assume that the hidden neutrons are not significantly diffused by the nuclei of gas molecules or atoms. In addition, absorption prevails on diffusion processes ( $\sigma_I \gg \sigma_E$  in helium-3 or BF<sub>3</sub>).

detectors we simply get the intuitive but not so obvious result

$$\Gamma \sim (1/2)pn\sigma_I V \Phi_-, \quad (\text{B14})$$

where  $V = S_d L$  is the volume of the detector and  $n\sigma_I = \Sigma_A$  is the macroscopic absorption cross section of the gas.

- 
- [1] K. Akama, *Pregeometry*, Lect. Notes Phys. **176** (1983) 267, arXiv:hep-th/0001113;  
V.A. Rubakov, M.E. Shaposhnikov, *Do we live inside a domain wall?*, Phys. Lett. **125B** (1983) 136;  
M. Pavsic, *Einstein's gravity from a first order lagrangian in an embedding space*, Phys. Lett. **116A** (1986) 1, arXiv:gr-qc/0101075;  
P. Horava, E. Witten, *Heterotic and Type I String Dynamics from Eleven Dimensions*, Nucl. Phys. **B460** (1996) 506, arXiv:hep-th/9510209;  
A. Lukas, B.A. Ovrut, K.S. Stelle, D. Waldram, *The Universe as a Domain Wall*, Phys. Rev. D **59** (1999) 086001, arXiv:hep-th/9803235;  
R. Davies, D. P. George, R. R. Volkas, *The standard model on a domain-wall brane?*, Phys. Rev. D **77** (2008) 124038, arXiv:0705.1584 [hep-ph].
- [2] P. Brax, C. van de Bruck, A.-C. Davis, *Brane world cosmology*, Rep. Prog. Phys. **67** (2004) 2183-2231, arXiv:hep-th/0404011;  
P. Brax, C. van de Bruck, *Cosmology and brane worlds: a review*, Class. Quantum Grav. **20** (2003) R201-R232, arXiv:hep-th/0303095;  
R. Dick, *Brane worlds*, Class. Quantum Grav. **18** (2001) R1-R23, arXiv:hep-th/0105320.
- [3] I. Antoniadis, N. Arkani-Hamed, S. Dimopoulos, G. Dvali, *New dimensions at a millimeter to a Fermi and superstrings at a TeV*, Phys. Lett. B **436** (1998) 257, arXiv:hep-ph/9804398;  
N. Arkani-Hamed, S. Dimopoulos, G. Dvali, *Phenomenology, Astrophysics and Cosmology of Theories with Sub-Millimeter Dimensions and TeV Scale Quantum Gravity*, Phys. Rev. D **59** (1999) 086004, arXiv:hep-ph/9807344.
- [4] D. Hooper, S. Profumo, *Dark Matter and Collider Phenomenology of Universal Extra Dimensions*, Phys. Rep. **453** (2007) 29, arXiv:hep-ph/0701197.
- [5] J.A.R. Cembranos, R. L. Delgado, A. Dobado, *Brane worlds at the LHC: Branons and KK gravitons*, Phys. Rev. D **88**, 075021 (2013).
- [6] I. Antoniadis, S. Baessler, M. Büchner, V.V. Fedorov,

- S. Hoedl, A. Lambrecht, V.V. Nesvizhevsky, G. Pignol, K.V. Protasov, S. Reynaud, Yu. Sobolev, *Short-range fundamental forces*, C. R. Physique **12** (2011) 755-778.
- [7] J. Redondo, A. Ringwald, *Light shining through walls*, Contemp. Phys. **52** (2011) 211-236, arXiv:1011.3741 [hep-ph].
- [8] S.N. Gninenko, *Search for MeV dark photons in a light-shining-through-walls experiment at CERN*, Phys. Rev. D **89** (2014) 075008, arXiv:1308.6521 [hep-ph].
- [9] S.N. Gninenko, N.V. Krasnikov, V.A. Matveev, *Invisible decay of muonium: Tests of the standard model and searches for new physics*, Phys. Rev. D **87** (2013) 015016, arXiv:1209.0060 [hep-ph].
- [10] S.N. Gninenko, *Search for invisible decays of  $\pi^0$ ,  $\eta$ ,  $\eta'$ ,  $K_S$  and  $K_L$ : A probe of new physics and tests using the Bell-Steinberger relation*, Phys. Rev. D **91** (2015) 015004, arXiv:1409.2288 [hep-ph].
- [11] H. Abele, *The neutron. Its properties and basic interactions*. Prog. Part. Nucl. Phys. **60** (2008) 1.
- [12] M. Sarrazin, F. Petit, *Equivalence between domain walls and "noncommutative" two-sheeted spacetimes: Model-independent matter swapping between branes*, Phys. Rev. D **81**, 035014 (2010), arXiv:0903.2498 [hep-th].
- [13] F. Petit, M. Sarrazin, *Quantum dynamics of massive particles in a non-commutative two-sheeted space-time*, Phys. Lett. B **612**, 105 (2005), arXiv:hep-th/0409084.
- [14] M. Sarrazin, F. Petit, *Brane matter, hidden or mirror matter, their various avatars and mixings: many faces of the same physics*, Eur. Phys. J. C **72** (2012) 2230, arXiv:1208.2014 [hep-ph].
- [15] M. Sarrazin, F. Petit, *Matter localization and resonant deconfinement in a two-sheeted spacetime*, Int. J. Mod. Phys. A **22**, 2629 (2007), arXiv:hep-th/0603194.
- [16] M. Sarrazin, F. Petit, *Laser frequency combs and ultracold neutrons to probe braneworlds through induced matter swapping between branes*, Phys. Rev. D **83**, 035009 (2011), arXiv:0809.2060 [hep-ph].
- [17] M. Sarrazin, G. Pignol, F. Petit, V.V. Nesvizhevsky, *Experimental limits on neutron disappearance into another braneworld*, Phys. Lett. B **712** (2012) 213, arXiv:1201.3949 [hep-ph].
- [18] S. Baessler, V.V. Nesvizhevsky, K.V. Protasov, A.Yu. Voronin, *Constraint on the coupling of axionlike particles to matter via an ultracold neutron gravitational experiment*, Phys. Rev. D **75**, 075006 (2007), arXiv:hep-ph/0610339.
- [19] I. Altarev, C.A. Baker, G. Ban, K. Bodek, M. Daum, P. Fierlinger, P. Geltenbort, K. Green, M.G.D. van der Grinten, E. Gutmiedl, P.G. Harris, R. Henneck, M. Horras, P. Iaydjiev, S. Ivanov, N. Khomutov, K. Kirch, S. Kistryn, A. Knecht, P. Knowles, A. Kozela, F. Kuchler, M. Kuz'niak, T. Lauer, B. Lauss, T. Lefort, A. Mtchedlishvili, O. Naviliat-Cuncic, S. Paul, A. Pazgalev, J.M. Pendlebury, G. Petzoldt, E. Pierre, C. Plonka-Spehr, G. Quémener, D. Rebreyend, S. Roccia, G. Rogel, N. Severijns, D. Shiers, Yu. Sobolev, R. Stoepfer, A. Weis, J. Zejma, J. Zenner, G. Zsigmond, *Neutron to Mirror-Neutron Oscillations in the Presence of Mirror Magnetic Fields*, Phys. Rev. D **80**, 032003 (2009), arXiv:0905.4208 [nucl-ex]; A.P. Serebrov, E.B. Aleksandrov, N.A. Dovator, S.P. Dmitriev, A.K. Fomin, P. Geltenbort, A.G. Kharitonov, I.A. Krasnoschekova, M.S. Lasakov, A.N. Murashkin, G.E. Shmelev, V.E. Varlamov, A.V. Vassiljev, O.M. Zherebtsov, O. Zimmer, *Experimental search for neutron - mirror neutron oscillations using storage of ultracold neutrons*, Phys. Lett. B **663**, 181 (2008), arXiv:0706.3600 [nucl-ex]; G. Ban, K. Bodek, M. Daum, R. Henneck, S. Heule, M. Kasprzak, N. Khomutov, K. Kirch, S. Kistryn, A. Knecht, P. Knowles, M. Kuzniak, T. Lefort, A. Mtchedlishvili, O. Naviliat-Cuncic, C. Plonka, G. Quémener, M. Rebetez, D. Rebreyend, S. Roccia, G. Rogel, M. Tur, A. Weis, J. Zejma, G. Zsigmond, *Direct Experimental Limit on Neutron Mirror-Neutron Oscillations*, Phys. Rev. Lett. **99**, 161603 (2007), arXiv:0705.2336 [nucl-ex].
- [20] Y.N. Pokotilovski, *On the experimental search for neutron - mirror neutron oscillations*, Phys. Lett. B **639** (2006) 214-217, arXiv:nucl-ex/0601017.
- [21] Z. Berezhiani, *More about neutron - mirror neutron oscillation*, Eur. Phys. J. C **64** (2009) 421, arXiv:0804.2088 [hep-ph]; Z. Berezhiani, L. Bento, *Neutron-Mirror Neutron Oscillations: How Fast Might They Be?*, Phys. Rev. Lett. **96** (2006) 081801, arXiv:hep-ph/0507031.
- [22] R.N. Mohapatra, S. Nasri, S. Nussinov, *Some Implications of Neutron Mirror Neutron Oscillation*, Phys. Lett. B **627** (2005) 124, arXiv:hep-ph/0508109.
- [23] G. Dvali, M. Redi, *Phenomenology of  $10^{32}$  Dark Sectors*, Phys. Rev. D **80** (2009) 055001, arXiv:0905.1709 [hep-ph].
- [24] A.T. Yue, M.S. Dewey, D.M. Gilliam, G.L. Greene, A.B. Laptev, J.S. Nico, W.M. Snow, F.E. Wietfeldt, *Improved Determination of the Neutron Lifetime*, Phys. Rev. Lett. **111**, 222501 (2013), arXiv:1309.2623 [nucl-ex].
- [25] A. Coc, M. Pospelov, J.-P. Uzan, E. Vangioni, *Modified big bang nucleosynthesis with non-standard neutron sources*, Phys. Rev. D **90**, 085018 (2014), arXiv:1405.1718 [hep-ph].
- [26] R. Lakes, *Experimental Limits on the Photon Mass and Cosmic Magnetic Vector Potential*, Phys. Rev. Lett. **80**, 1826 (1998); J. Luo, C.-G. Shao, Z.-Z. Liu, Z.-K. Hu, *Determination of the limit of photon mass and cosmic magnetic vector with rotating torsion balance*, Phys. Lett. A **270**, 288 (2000).
- [27] G. Feinberg, S. Weinberg, *Conversion of muonium into antimuonium*, Phys. Rev. **123**, 1439 (1961).
- [28] S.V. Demidov, D.S. Gorbunov, A.A. Tokareva, *Positronium oscillations to Mirror World revisited*, Phys. Rev. D **85**, 015022 (2012), arXiv:1111.1072 [hep-ph].
- [29] D. Ridikas, G. Fioni, P. Goberis, O. Deruelle, M. Fadil, F. Marie, S. Röttger, *On the fuel cycle and neutron fluxes of the high flux reactor at ILL Grenoble*, Proc. of the 5th Int. Specialists' meeting SATIF-5, OECD/NEA Paris (2000).
- [30] V.V. Nesvizhevsky, E.V. Lychagin, A.Yu. Muzychka, G.V. Nekhaev, A.V. Strelkov, *About interpretation of experiments on small increase in energy of UCN in traps*, Physics Letters B **479** (2000) 353.
- [31] E.V. Lychagin, A.Yu. Muzychka, V.V. Nesvizhevsky, G.V. Nekhaev, A.V. Strelkov, *Experimental estimation of the possible subbarrier penetration of ultracold neutrons through vacuum-tight foils*, JETP Letters **71** (2000) 447.
- [32] V.V. Nesvizhevsky, H.G. Boerner, A.M. Gagarski, A.K. Petoukhov, G.A. Petrov, H. Abele, S. Baessler, G. Divkovic, F.J. Ruess, T. Stoeflerle, A. Westphal, A.V. Strelkov, K.V. Protasov, A.Yu. Voronin, *Measurement of quantum states of neutrons in the Earth's*

*gravitational field*, Phys. Rev. D **67** (2003) 102002, arXiv:hep-ph/0306198.

[33] A.-J. Dianoux, G. Lander, *Neutron Data Booklet*, (OCP Science, 2003).